PRAMANA
— journal of
physics

Vol. 85, No. 5
November 2015
pp. 929–945

A Hamiltonian approach to model and analyse networks of nonlinear oscillators: Applications to gyroscopes and energy harvesters

PIETRO-LUCIANO BUONO[1], BERNARD CHAN[2], ANTONIO PALACIOS[2,*] and VISARATH IN[3]

[1]Faculty of Science, University of Ontario Institute of Technology, 2000 Simcoe St N, Oshawa, ON L1H 7K4, Canada
[2]Nonlinear Dynamical Systems Group, Department of Mathematics, San Diego State University, San Diego, CA 92182, USA
[3]Space and Naval Warfare Systems Center, Code 71730 53560 Hull Street, San Diego, CA 92152-5001, USA
*Corresponding author. E-mail: palacios@euler.sdsu.edu

DOI: 10.1007/s12043-015-1079-4; ***e*Publication:** 24 September 2015

Abstract. Over the past twelve years, ideas and methods from nonlinear dynamics system theory, in particular, group theoretical methods in bifurcation theory, have been used to study, design, and fabricate novel engineering technologies. For instance, the existence and stability of heteroclinic cycles in coupled bistable systems has been exploited to develop and deploy highly sensitive, low-power, magnetic and electric field sensors. Also, patterns of behaviour in networks of oscillators with certain symmetry groups have been extensively studied and the results have been applied to conceptualize a multifrequency up/down converter, a channelizer to lock into incoming signals, and a microwave signal generator at the nanoscale. In this manuscript, a review of the most recent work on modelling and analysis of two seemingly different systems, an array of gyroscopes and an array of energy harvesters, is presented. Empirical values of operational parameters suggest that damping and external forcing occur at a lower scale compared to other parameters, so that the individual units can be treated as Hamiltonian systems. Casting the governing equations in Hamiltonian form leads to a common approach to study both arrays. More importantly, the approach yields analytical expressions for the onset of bifurcations to synchronized oscillations. The expressions are valid for arrays of any size and the ensuing synchronized oscillations are critical to enhance performance.

Keywords. Gyroscopes; energy harvesters; synchronization; Hamiltonian mechanics.

PACS Nos 02.50.Ey; 05.10.Gg; 05.40.−a; 85.70.Ay

1. Introduction

The seminal work of William Rowan Hamilton in the 19th century [1,2] led to a novel reformulation of Newton's equations in terms of canonical coordinates that account for the position and momentum of a mechanical system. Hamilton formulation was novel because it presented a unified framework to model and analyse physical and mechanical systems described by ordinary differential equations, partial differential equations or through calculus of variations. Along the way, the concept of integrable systems was conceived to describe nonlinear differential equations that admit an analytic solution.

Nowadays, integrable systems arise naturally at various length scales: in molecular dynamics [3], underwater vehicle dynamics [4], in magnetic- and electric-field sensors [5–8], hydroelastic rotating systems and boats/ships [9–12], in complex systems such as telecommunication infrastructures [13], and in power grids [14]. In this manuscript we present a review of the analysis of two seemingly unrelated arrays of N mechanical systems: one of vibratory gyroscopes [12,15–17] and the other of energy harvester devices [18,19]. The rationale for coupling is to exploit the emergence of collective synchronized oscillations to optimize the performance: reduce phase drift induced by noise in the case of gyroscopes and increase power output for energy harvesters. The specific choice of coupling in each system is dictated by experimental works. That is, for the array of gyroscopes, the natural choice is bidirectionally through the driving axes of each gyroscope, leading to an array with dihedral $\mathbf{D}_N$. For the array of energy harvesting, the experimental implementation is based on placing multiple composite beams on a common vibration base, which in this case yields all-to-all coupling represented by the group $\mathbf{S}_N$ of permutations of N objects. Other choices, for instance, unidirectional coupling, can lead to arrays that do not preserve the Hamiltonian structure of each unit. In other words, spatial symmetry alone is not a necessary and sufficient condition for an array to retain a Hamiltonian structure as a network. Nevertheless, the groups $\mathbf{D}_N$ and $\mathbf{S}_N$ do preserve the Hamiltonian structure, so that the ideas and methods in this review article can be readily extended to other systems. Under empirical parameter values produced by experiments, dissipative and external forcing might be negligible, so that each individual unit can be treated as an integrable Hamiltonian dynamical system of dimensions 4. Collectively, the governing equations of each array lead to a non-autonomous system of ordinary differential equations of dimensions $4N$.

From an engineering standpoint, these two systems, the gyroscopes and the energy harvesters, could not be more different. Gyroscopes are designed to measure angular rates of rotations and their performance depends on minimizing phase drift in the oscillations of the sensing axes. Energy harvesters are manufactured to store electrical current or voltage and their performance is measured by maximizing the power output. From a mathematical point of view, the systems are, however, very similar. The normal forms of the governing equations consist of non-autonomous equations of the Duffing-type and the phase space is identical, i.e., $\mathbb{R}^{4N}$. Due to these similarities, we employ a common approach to study their collective behaviour. First, the governing equations, without forcing and damping, are reformulated in a Hamiltonian structure. Then the isotypic decomposition of the phase space $\mathbb{R}^{4N}$ under the action of the group of symmetries, $\mathbf{D}_N$ for gyroscopes and $\mathbf{S}_N$ for energy harvesters, are used to study the linearized system of equations. This approach allows us to calculate approximate analytical expressions for the critical value of coupling

strength that leads to synchronized oscillations in each system. The expressions are reasonable approximations for weak forcing and small damping, under which the branches of equilibrium states become foliated by periodic oscillations. They are valid for any network of size N and remain valid under non-zero weak coupling. More importantly, they can be used to design and tune-up future experimental works.

2. Gyroscope system

In recent years, we have discovered [20] that coupling of similar vibratory gyroscopes can lead to a new concept of a N degrees-of-freedom (DOF) coupled inertial navigation system, with the ability to minimize the effects of noise, material imperfections, phase drift, and power consumption significantly more than any single device. Experimental works reveal that damping and forcing coefficients have a relatively small scale compared to other system parameters. Thus, the equations can be written as a Hamiltonian system and the dynamics can be studied as perturbations of the Hamiltonian structure. In this section, we review this approach and the calculations that lead to an analytical approximation for the onset of synchronized oscillations, which are critical to the operation of the device.

2.1 *Vibratory gyroscopes*

A conventional vibratory gyroscope consists of a proof-mass system as shown in figure 1. The system operates [21–23] on the basis of energy transferred from a driving mode to a sensing mode through the Coriolis force [24]. In this configuration, a change in acceleration around the driving x-axis caused by the presence of the Coriolis force induces

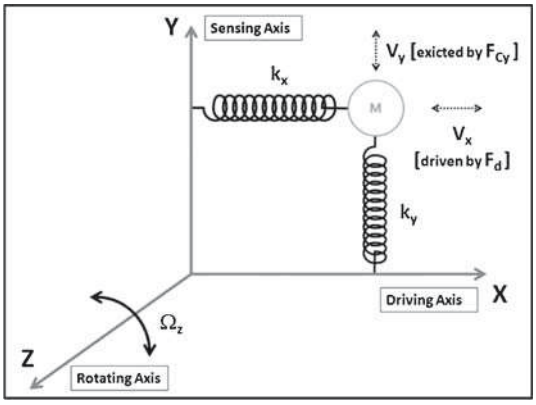

Figure 1. Schematic diagram of a vibratory gyroscope system. An internal driving force induces the spring-mass system to vibrate in one direction, the x-axis in this example. An external rotating force, perpendicular to the xy-plane induces oscillations in the y-direction by transferring energy through the Coriolis force. These latter oscillations can be used to detect and quantify the rate of rotation.

a vibration in the sensing y-axis which can be converted to measure angular rate output or absolute angles of rotation. The governing equations of the gyroscope can be written as

$$\begin{aligned} m\ddot{x} + c_x\dot{x} + \kappa_x x + \mu_x x^3 &= f_e(t) + 2m\Omega_z\dot{y}, \\ m\ddot{y} + c_y\dot{y} + \kappa_y y + \mu_y y^3 &= -2m\Omega_z\dot{x}, \end{aligned} \tag{1}$$

where x (y) represents the drive (sense) modes, m is the proof mass, Ω_z is the angular rate of rotation along a perpendicular direction (z-axis), c_x (c_y) is the damping coefficient along the x- (y-) direction, and κ_x (κ_y) and μ_x (μ_y) are the linear and nonlinear damping coefficients along the x- (y-) directions, respectively. Typically, the forcing term has a sinusoidal form $f_e(t) = A_d \cos w_d t$, where A_d is the amplitude and w_d is the frequency of the excitation. The Coriolis forces appear in the driving and sensing modes as $F_{cx} = 2m\Omega_z\dot{y}$ and $F_{cy} = -2m\Omega_z\dot{x}$, respectively.

2.2 *A ring of coupled gyroscopes with dihedral symmetry*

We now consider N identical gyroscopes coupled identically in a ring system, with no preferred direction leading to $\mathbf{D}_N$ symmetry, as shown in figure 2. We assume that $\mu_x = \mu_y = \mu > 0$, mainly to reduce the complexity in dealing with nonlinear terms. Nevertheless, the results should still hold for relatively small variations in parameter values but a complete analysis of non-identical gyroscope systems is beyond the scope of the present work. Thus, the behaviour of the individual ith gyroscope in the system, with identical coupling strength λ is described by the following system of differential equations:

$$\begin{aligned} m\ddot{x}_i + c_x\dot{x}_i + \kappa_x x_i + \mu x_i^3 &= f_e(t) + 2m_i\Omega\dot{y}_i + \lambda\sum_{i=1}^{N}(x_{i-1} - 2x_i + x_{i+1}), \\ m\ddot{y}_i + c_y\dot{y}_i + \kappa_y y_i + \mu y_i^3 &= -2m_i\Omega\dot{x}_i. \end{aligned} \tag{2}$$

We now rewrite the governing equations (2) as a first-order system of differential equations. Let $q_i = (q_{i1}, q_{i2})^T = (x_i, y_i)^T$ be the configuration components and $p_i = m\dot{q}_i + Gq_i$ be the momentum components of a single gyroscope, where

$$G = \begin{pmatrix} 0 & -m\Omega \\ m\Omega & 0 \end{pmatrix}.$$

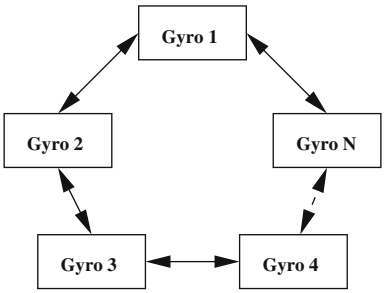

Figure 2. Schematic diagram of a ring of coupled vibratory gyroscopes with no preferred direction of coupling, i.e., bidirectional, exhibiting $\mathbf{D}_N$ symmetry.

Directly differentiating the momentum components, we get (after rearranging terms) $m\ddot{q}_i = \dot{p}_i - G\dot{q}_i$. Then the original equations (2), which have total phase space $\mathbb{R}^{4N}$, can be written in the following form: Letting $Z_i = (q_i, p_i)$, the internal dynamics of each individual ith gyroscope can be expressed as follows:

$$\mathcal{F}(Z_i) = \begin{pmatrix} -G/m & (1/m)I_2 \\ -(GF/m)+K-(1/m)G^2 & (1/m)(F-G) \end{pmatrix} \begin{pmatrix} q_i \\ p_i \end{pmatrix} + \begin{pmatrix} 0 \\ -f_i \end{pmatrix},$$

with $F = \mathrm{diag}(c_x, c_y)$, $K = \mathrm{diag}(\kappa_x, \kappa_y)$, and $f_i = \mu(q_{i1}^3, q_{i2}^3)^T$. Then the governing equations of the $\mathbf{D}_N$ symmetric ring can be written as

$$\frac{\mathrm{d}Z_i}{\mathrm{d}t} = \mathcal{F}(Z_i) + \mathcal{H}(Z_{i+1}, Z_i) + \mathcal{H}(Z_{i-1}, Z_i) + R(t), \tag{3}$$

where $R(t) = (0, f_e(t), 0, 0)^T$,

$$\mathcal{H}(Z_{i+1}, Z_i) = \begin{pmatrix} 0 \\ \lambda\Gamma(q_{i+1} - q_i) \end{pmatrix} \quad \text{and} \quad \Gamma = \begin{pmatrix} 1 & 0 \\ 0 & 0 \end{pmatrix}.$$

Note that as the nonlinear terms are given only by cubic terms, each gyroscope is symmetric with respect to the $-I$ transformation $(q_i, p_i) \to (-q_i, -p_i)$. Because the coupling is also symmetric with respect to this $\mathbf{Z}_2(-I)$-symmetry, that is, $\mathcal{H}(-Z_{i+1}, -Z_i) = -\mathcal{H}(Z_{i+1}, Z_i)$, then the networks have symmetry group given by the direct product of the network symmetry and the $\mathbf{Z}_2(-I)$ symmetry, i.e., $\mathbf{D}_N(\gamma, \eta) \times \mathbf{Z}_2(-I)$ (see Dionne *et al.* [25] for details).

2.3 *Hamiltonian structure of the unforced, $f_e(t) = 0$, ring*

For the remainder of the paper we assume that $c_x = c_y = 0$. Each uncoupled gyroscope has phase space $\mathbb{R}^4$, so that we define the symplectic form

$$\omega_4(u, v) = u^T J_4 v, \quad J_{2n} = \begin{pmatrix} 0 & I_n \\ -I_n & 0 \end{pmatrix}, \tag{4}$$

with $u, v \in \mathbb{R}^4$ and n a positive integer. Then, direct calculations show that $\dot{Z}_i = \mathcal{F}(Z_i)$ is a Hamiltonian vector field with respect to the symplectic form ω_4, with Hamiltonian function

$$\begin{aligned} H(q_i, p_i) = &-\frac{1}{2}p_i^T\left(K - \frac{G^2}{m}\right)q_i - q_i^T\frac{G}{m}q_i + p_i^T\frac{G}{m}p_i \\ &+ q_i^T\frac{I_2}{m}p_i + H_2(q_i, p_i), \end{aligned}$$

where $H_2(q_i, p_i) = (\mu/4)(q_{i1}^4 + q_{i2}^4)$. We now address the question of whether the coupled system is also Hamiltonian with respect to the symplectic structure

$$J = \mathrm{diag}\,\underbrace{(J_4, \ldots, J_4)}_{N \text{ times}}, \tag{5}$$

where J_4 is defined by (4). The linearized system can be written as

$$M_{\mathrm{bi}} = I_N \otimes M_1 + (C + C^T) \otimes M_2, \tag{6}$$

with M_1 and M_2 defined as follows:

$$M_1 = \begin{pmatrix} -(G/m) & (1/m)I_2 \\ -(K-(1/m)G^2+2\lambda\Gamma) & -(G/m) \end{pmatrix}, \quad M_2 = \begin{pmatrix} 0 & 0 \\ \lambda\Gamma & 0 \end{pmatrix},$$

Now, a matrix $B \in R^{2n}$ is Hamiltonian if it satisfies

$$B^T J_{2n} + J_{2n} B = 0. \tag{7}$$

We can check directly that M_1 and M_2 are Hamiltonian matrices with respect to J_4. Thus, all the linearized internal and coupling matrices are Hamiltonian, but we still need to verify that the overall coupled linear systems are also Hamiltonian when coupled with their respective structure. Indeed, one can verify that $M_{\text{bi}}^T J + J M_{\text{bi}} = 0$ holds. Since both M_1 and M_2 are Hamiltonian with respect to J_4, the corresponding linear Hamiltonian function is

$$H(Z) = \frac{1}{2} Z^T J^T M_{\text{bi}} Z.$$

Hence, the Hamiltonian of the complete $\mathbf{D}_N$-symmetric ring can now be expressed in terms of position and momentum coordinates $(q, p) = (q_1, \ldots, q_N, p_1, \ldots, p_N)$ as

$$\begin{aligned} H(q,p) = \frac{1}{2}\sum_{i=1}^{N} -p_i^T \left(K - \frac{G^2}{m} + 2\lambda\Gamma\right) q_i - q_i^T \frac{G}{m} q_i + p_i^T \frac{G}{m} p_i + q_i^T \frac{I_2}{m} p_i \\ - (q_{i+1} + q_{i-1})^T \lambda\Gamma q_i + H_2(q,p). \end{aligned}$$

2.4 *Isotypic decomposition for* $\mathbf{D}_N$ *symmetry*

We now construct a symplectic linear transformation to decompose the system into its isotypic components, which allows us to write the linear part of the equations in block diagonal form and then simplify the stability analysis. For $\zeta = \exp(2\pi i/N)$ and some $v \in \mathbb{R}$, let $v_j = (v, \zeta^j v, \zeta^{2j} v, \ldots, \zeta^{(N-1)j} v)^T$ be a vector in $\mathbb{C}$. Suppose $j = 0, \ldots, N-1$, then the vectors v_j form a basis for $\mathbb{C}^N$, that is

$$\left(\mathbb{C}^N\right)^4 = V_0^4 \oplus V_1^4 \oplus \cdots \oplus V_{N-1}^4, \tag{8}$$

where $V_j = \mathbf{C}\{v_j\}$ are invariant subspaces. Given that each vibratory gyroscope has an internal phase space of dimension four, let

$$e_1 = \begin{pmatrix} 1 \\ 0 \\ 0 \\ 0 \end{pmatrix}, \quad e_2 = \begin{pmatrix} 0 \\ 1 \\ 0 \\ 0 \end{pmatrix}, \quad e_3 = \begin{pmatrix} 0 \\ 0 \\ 1 \\ 0 \end{pmatrix}, \quad e_4 = \begin{pmatrix} 0 \\ 0 \\ 0 \\ 1 \end{pmatrix},$$

be the canonical basis of $\mathbb{R}^4$ and define $v_{ji} = (e_i, \zeta^j e_i, \zeta^{2j} e_i, \ldots, \zeta^{(N-1)j} e_i)^T$, for $i = 1, 2, 3, 4$. Direct calculations show that this set of $4N$ vectors form a symplectic basis under the symplectic form $\omega(u, v) = u^T J v$, with $u, v \in \mathbb{C}^{4N}$ and J given by (4), so that $\omega(v_{ji}, v_{k\ell}) = 0$ holds for any pair $v_{ji}, v_{k\ell}$ in the basis of $\mathbb{C}^{4N}$. The corresponding real symplectic transition matrix P is constructed as follows: For a complex vector v_{ji}, let

$\Re_{ji}$ and $\Im_{ji}$ denote its real and imaginary parts, respectively. Furthermore, we denote a normalized vector by $\tilde{\cdot}$. For N odd, the real symplectic transition matrix is

$$P = \left[\tilde{v}_{01}, \ldots, \tilde{v}_{04}, \widetilde{\Im}_{11}, \widetilde{\Re}_{11}, \ldots, \widetilde{\Im}_{14}, \widetilde{\Re}_{14}, \ldots, \widetilde{\Im}_{\lfloor N/2\rfloor 1}, \widetilde{\Re}_{\lfloor N/2\rfloor 1}, \ldots, \widetilde{\Im}_{\lfloor N/2\rfloor 4}, \widetilde{\Re}_{\lfloor N/2\rfloor 4}\right].$$

Similarly, the corresponding real symplectic matrix for N even is

$$P = \left[\tilde{v}_{01}, \ldots, \tilde{v}_{04}, \widetilde{\Im}_{11}, \widetilde{\Re}_{11}, \ldots, \widetilde{\Im}_{14}, \widetilde{\Re}_{14}, \ldots, \widetilde{\Im}_{(N/2-1)1}, \widetilde{\Re}_{(N/2-1)1}, \ldots, \widetilde{\Im}_{(N/2-1)4}, \widetilde{\Re}_{(N/2-1)4}, \tilde{v}_{(N/2)1}, \ldots, \tilde{v}_{(N/2)4}\right].$$

From the basis chosen, the complexified phase space can now be written as

$$\left(\mathbb{C}^N\right)^4 = V_0^4 \oplus V_1^4 \oplus \cdots \oplus V_{N-1}^4.$$

Applying P to the linear part of (3) we obtain the system in its block diagonal form $P^{-1}MP = \mathcal{M}$. For N odd, $\mathcal{M} = \text{diag}\left(\mathcal{M}_0, \mathcal{M}_1, \mathcal{M}_1, \ldots, \mathcal{M}_{\lfloor N/2\rfloor}, \mathcal{M}_{\lfloor N/2\rfloor}\right)$, and for N even $\mathcal{M} = \text{diag}\left(\mathcal{M}_0, \mathcal{M}_1, \mathcal{M}_1, \ldots, \mathcal{M}_{N/2-1}, \mathcal{M}_{N/2-1}, \mathcal{M}_{N/2}\right)$, where $\mathcal{M}_j = M_1 + 2\cos(2\pi j/N)M_2$.

2.5 *Linear stability*

We now calculate the eigenvalues of the matrix $\mathcal{M}$. Since the linear system is in block diagonal form, the eigenvalues are the same as the combined eigenvalues of all the $\mathcal{M}_j$ blocks. Of the four eigenvalues, two of them have the form

$$\rho_j^{\pm} = \frac{1}{\sqrt{m}}\sqrt{-\left(\kappa + 2m\Omega^2 + \lambda\left(1 - \cos\left(2\pi j/N\right)\right)\right) \pm \sqrt{s_j}},$$

where $s_j = 4m\Omega^2(\kappa + m\Omega^2 + \lambda(1 - \cos(2\pi j/N))) + \lambda^2(1 - \cos(2\pi j/N))^2$. The other two eigenvalues are $-\rho_j^{\pm}$. It is straightforward to check that because $\kappa > 0$, the eigenvalue ρ_j^- is purely imaginary for all $\lambda \in \mathbb{R}$. Observe that $\rho_j^+ = 0$, if and only if, $\kappa + 2\lambda(1 - \cos(2\pi j/N)) = 0$, that is,

$$\lambda_j^* = -\frac{\kappa}{2(1 - \cos(2\pi j/N))}. \tag{9}$$

This result implies that λ_j^* is maximum when $j = \lfloor N/2\rfloor$. For N even, $\lambda_{\lfloor N/2\rfloor}^* = -\kappa/4$ and for N odd, $\lambda_{\lfloor N/2\rfloor}^*$ takes its smallest value for $N = 3$ at $-\kappa/3$ and converges to $-\kappa/4$ as $N \to \infty$.

One can easily check that as λ increases through λ_j^*, ρ_j^+ changes from real to purely imaginary. Thus, for $\lambda > \lambda_{\lfloor N/2\rfloor}^*$ all eigenvalues are purely imaginary.

Next we establish the relationship between equilibrium solutions of the unforced system with periodic solutions of the forced system with the small coupling parameter A. Then we conclude this section by stating the threshold condition that leads to the emergence of stable synchronized oscillations in the ring dynamics.

2.6 *Emergence of synchronized oscillations under forcing*

We consider again the governing equations for the bidirectional ring (without forcing) written as a separation of linear M and nonlinear terms, that is

$$\frac{\mathrm{d}Z}{\mathrm{d}t} = MZ + F(Z), \tag{10}$$

where again: $Z = (Z_1, \ldots, Z_N)^T$, $Z_i = (q_i, p_i)^T$, $F = (F_1, \ldots, F_N)^T$, and $F_i = (0, -f_i)^T$ with $i = 1, \ldots, N \bmod N$. Also, recall that $M = M_{\text{bi}}$. Let $\tau = t$ and now write the system in extended phase space

$$\frac{\mathrm{d}Z}{\mathrm{d}t} = MZ + F(Z) + H_A(\tau) := S(Z, \tau, A), \quad \frac{\mathrm{d}\tau}{\mathrm{d}t} = 1, \tag{11}$$

where

$$H_A(\tau) = \underbrace{(\underbrace{0, f_e(\tau), 0, 0}, \ldots, \underbrace{0, f_e(\tau), 0, 0})}_{N \text{ times}}.$$

We can now establish, through the following proposition, the relationship between equilibrium solutions of the unforced system and periodic solutions of the forced system with the small coupling parameter A.

PROPOSITION 2.1

For the forcing frequency $\omega \in \mathbb{R}\backslash\{$a finite number of points$\}$, equilibrium solutions of the unforced system (10) *are in one-to-one correspondence with $2\pi/\omega$-periodic solutions of* (11)*. Moreover*,

(1) *If Z_0 is an equilibrium solution of* (10) *with isotropy subgroup Σ, then the corresponding periodic solution $P_0(t)$ has spatial isotropy subgroup Σ.*
(2) *Z_0 is spectrally stable/strongly stable/unstable, if and only if, $P_0(t)$ is spectrally stable/strongly stable/unstable.*

Next we introduce the main result of this section, i.e., a theorem that describes the threshold value for the emergence of stable synchronized oscillations.

Theorem 2.2. *If the forcing parameter A is small enough, system* (11) *with bidirectional coupling has a fully synchronized $2\pi/\omega$-periodic solution $\tilde{Z}(t)$ near Z_0 with isotropy subgroup $\mathbf{D}_N \times \mathbf{Z}_2$, strongly stable for*

$$\lambda > \lambda^* = -\frac{\kappa}{2(1 - \cos(2\pi \lfloor N/2 \rfloor / N))}. \tag{12}$$

For N even, $\lambda^*_{N/2}$ is the threshold value for a bifurcation from the $\mathcal{M}_{N/2}$ block and so a single pair of eigenvalues crosses the origin. For N odd, $\lambda^*_{\lfloor N/2 \rfloor}$ is the threshold value for a bifurcation from the two $\mathcal{M}_{\lfloor N/2 \rfloor}$ blocks and thus a double pair of eigenvalues crosses the origin. Observe that the term $f_e(t)$ from (2) does not play a role in the linear part of the system and so it does not affect the calculation of the eigenvalues. Consequently, excluding damping terms, $\lambda^*_{N/2}$ represents an analytical expression to the critical coupling strength that leads the gyroscopes into complete synchronization when the periodic forcing term $f_e(t)$ is added [26].

Observe that for the special case of a ring with $N = 3$ gyroscopes, eq. (12) yields $\lambda^* = -\kappa/3$. Based on related experimental work [20,27], we set $\kappa = 2.6494$ N/m to

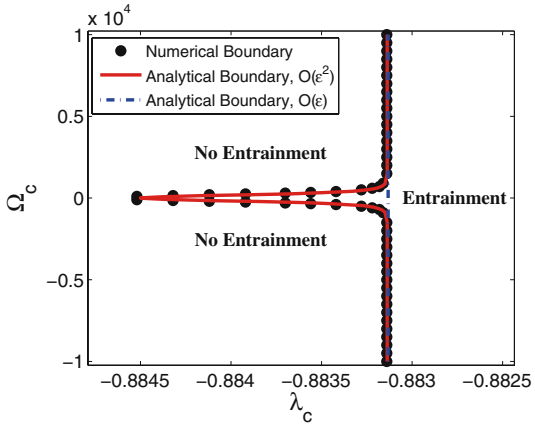

Figure 3. Two-parameter bifurcation diagram showing the region of parameter space (Ω, λ) where the vibrations of a system of three gyroscopes, coupled bidirectionally, become completely synchronized. The boundary curve is the locus of the pitchfork bifurcation where three periodic solutions of eq. (11) merge into a $\mathbf{D}_3 \times \mathbf{Z}_2$ symmetric one as the complete synchronization state becomes locally asymptotically stable.

get $\lambda^* = -0.8831$. This value fits very well with the almost vertical line threshold, in parameter space (Ω, λ), which was originally obtained through asymptotic methods [20], and reproduced in figure 3. The only difference is the cusp shape, which is due to the effect of damping. Recall that damping has been neglected in our analysis to preserve the Hamiltonian structure of the cells and of the network. Nevertheless, that cusp region is extremely small considering the scale along the λ-axis. Proofs of this proposition and theorem, together with details of the Birkhoff normal form analysis of nonlinear terms, can be found in [28].

3. Energy harvesting

The goal of all energy harvesting devices is to convert ambient or environmental energy into electrical energy [18,19,29]. A major disadvantage of these technologies is the fact that the amount of electrical energy produced is small. In response, a wide range of techniques that combine linear and nonlinear components with novel materials and coupling configurations have been proposed with the ultimate goal of harvesting more energy along a broad bandwidth of frequencies. In this section, we review the results of the investigation of a particular network-based energy harvesting system consisting of multiple, N-resonators, coupled mechanically and inductively in a ring configuration. The governing equations of the coupled system lead to a system of differential equations with all-to-all coupling between transducers. The normal forms are similar to those of the gyroscope with the exception of the symmetry group. Consequently, a similar approach based on Hamiltonian mechanics is employed to study the collective behaviour of the network.

3.1 *Beam model*

Figure 4a shows a schematic design of a coupled energy harvesting system with two possible coupling topologies, all-to-all and nearest neighbours. Each composite beam consisting of aluminum as the substrate, galfenol (FeGa) as the magnetostrictive material and magnet wire as coil is used to convert the mechanical vibrations into electrical voltage (see figure 4b). Galfenol was chosen in this work for its durability, compared to the brittleness often encountered with piezoelectric materials, and high magnetomechanical coupling. The AC signal is then fed into a rectifier and a related power converter circuit that stores the DC voltage in a thin film battery. The battery is used to power a low-power transmitter to send the sensor data intermittently and/or as sensing events take place. Next we analyse the collective response of the ring with the objective of maximizing power output through synchronized vibrations.

We assume a mesoscale implementation so that inductance coupling is negligible. Then the model equation for the ring vibrations can be written as

$$\frac{\mathrm{d}^2 z_j}{\mathrm{d}t^2} + 2\delta\frac{\mathrm{d}z_j}{\mathrm{d}t} + \omega_0^2 z_j + \frac{k_3}{m}z_j^3 + \frac{\lambda}{m}\sum_{k=1}^{N} z_k = \frac{A_\mathrm{d}}{m}\cos(w_\mathrm{d}t) - \frac{GC_L}{m}\frac{\mathrm{d}V_j}{\mathrm{d}t}$$

$$L_c C_L \frac{\mathrm{d}^2 V_j}{\mathrm{d}t^2} + C_L(R_L + R_c)\frac{\mathrm{d}V_j}{\mathrm{d}t} + V_j = G\frac{\mathrm{d}z_j}{\mathrm{d}t}, \tag{13}$$

where $z_j(t)$ is the displacement of the jth beam, in which $j = 1, \ldots, N$, with mass m, damping coefficient b, $2\delta = b/m$, linear and nonlinear coeffcients k_1 and k_3, respectively, natural frequency $w_0^2 = k_1/m$. The externally applied force is assumed to be sinusoidal, of the form $A_d \cos w_d t$, where A_d is the amplitude and w_d is the frequency of the excitation. In the readout coil, G is the transduction factor that measures the gain in the conversion of vibrations into electrical current, L_c and R_c are the coil inductance and resistance, respectively, and R_L is the load. Electrical current is converted to voltage

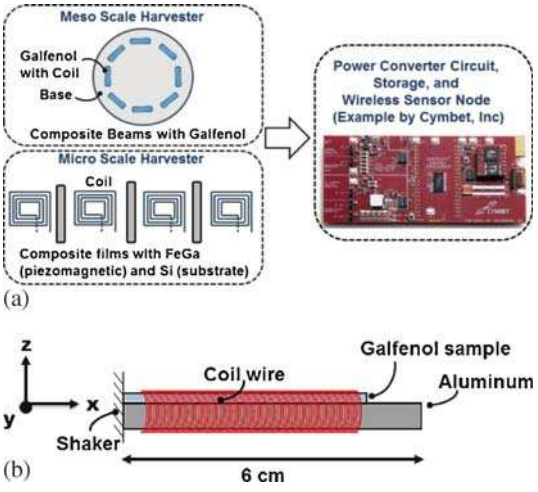

Figure 4. (**a**) Schematic design of a coupled energy harvesting system with all-to-all coupling and with nearest neighbours coupling. (**b**) Composite beams.

through a load capacitor with coefficient C_L. λ is the coupling strength, assumed to be identical throughout the ring.

Rescaling time and beam displacement and defining a dimensionless voltage through

$$V_j(t) = \frac{k_1\kappa}{C_L\omega_0 G}\sqrt{\frac{k_1}{|k_3|}}U_j(\tau),$$

yields the following equations in dimensionless form:

$$x_j''(\tau) + \frac{1}{Q}x_j'(\tau) + x_j(\tau) + \gamma x_j^3(\tau) + \lambda_r\sum_{k=1}^{N} x_k = F_r\cos(\omega_r\tau) - \kappa U_j'(\tau)$$

$$U_j''(\tau) + \alpha U_j'(\tau) + \beta U_j(\tau) = \kappa x_j'(\tau), \tag{14}$$

where $\beta = 1/(L_cC_L\omega_0^2)$. Note that now under this rescaling, the coefficient κ appears in front of both coupling derivative terms of eq. (14), which allows us to cast the equations in the Hamiltonian form.

3.2 *Hamiltonian formulation*

Disregarding damping terms and the period forcing in (14) without self-coupling, we may rewrite the governing equations for the ith energy harvester in vector form as

$$\begin{pmatrix} q_i' \\ p_i' \end{pmatrix} = \begin{pmatrix} -K & I_2 \\ \Lambda + K^2 & -K \end{pmatrix}\begin{pmatrix} q_i \\ p_i \end{pmatrix} - \begin{pmatrix} 0 \\ f_i + \lambda_r\sum_{j\to i}\Gamma q_j \end{pmatrix},$$

where

$$q_i = (q_{i1}, q_{i2})^T = (x_i, u_i)^T, \quad p_i = q_i' + Kq_i,$$

$$K = \frac{1}{2}\begin{pmatrix} 0 & \kappa \\ -\kappa & 0 \end{pmatrix}, \quad \Lambda = \begin{pmatrix} -1 & 0 \\ 0 & -\beta \end{pmatrix}, \quad f_i = \begin{pmatrix} \gamma x_i^3(\tau) \\ 0 \end{pmatrix}$$

and

$$\Gamma = \begin{pmatrix} 1 & 0 \\ 0 & 0 \end{pmatrix}.$$

Now, let

$$Y_i = (q_i, p_i)^T, \quad M_1 = \begin{pmatrix} -K & I_2 \\ \Lambda + K^2 & -K \end{pmatrix},$$

$$M_2 = \begin{pmatrix} 0 & 0 \\ -\lambda_r\Gamma & 0 \end{pmatrix} \quad \text{and} \quad F_i = \begin{pmatrix} 0 \\ -f_i \end{pmatrix},$$

then the equations for the entire ring can be written as

$$Y' = MY + F, \tag{15}$$

where

$$Y = \begin{pmatrix} Y_1 \\ Y_2 \\ \vdots \\ Y_N \end{pmatrix}, \quad M = \begin{pmatrix} M_1 & M_2 & \dots & \dots & M_2 \\ M_2 & M_1 & M_2 & \dots & M_2 \\ \vdots & \ddots & \ddots & & \vdots \\ \vdots & & \ddots & \ddots & \vdots \\ M_2 & \dots & & M_2 & M_1 \end{pmatrix}$$

and

$$F = \begin{pmatrix} F_1 \\ F_2 \\ \vdots \\ F_N \end{pmatrix}.$$

A direct calculation shows that the system in (15) is Hamiltonian with respect to the symplectic structure (5). The corresponding Hamiltonian is

$$H(Y(q_i, p_i)) = \frac{1}{2} Y^T J^{-1} M Y + \sum_{i=1}^{n} \gamma \frac{q_{i1}^4}{4}.$$

Next we study the linearized system near the origin starting with the $\mathbf{S}_N$ isotypic decomposition of the tangent space. This leads to a block diagonal decomposition from which the eigenvalues can be obtained explicitly and their distribution can be studied for all $N \in \mathbb{N}$. In particular, we determine for general N, a threshold condition for the origin to loose spectral stability as the coupling parameter λ is varied. The case with self-coupling is treated in a similar manner. Although results have been obtained for both cases, here only the details for the case without self-coupling has been included.

3.3 *Isotypic decomposition for* $\mathbf{S}_N$ *symmetry*

Let I_N denote the identity matrix in $\mathbb{R}^N$. We can write the generators of $\mathbf{S}_N$ in $\mathbb{R}^N$ as the set $\{\sigma_i : i = 1, \dots, N-1\}$, where σ_i is the matrix obtained by swapping columns i and $i+1$ of I_N. Since the phase space of the system is $\mathbb{R}^{4N}$, we can write its generators as

$$\xi = \{\xi_i = \sigma_i \otimes I_4 : i = 1, \dots, N-1\}.$$

For $\zeta = \exp(2\pi i/N)$ and some $v \in \mathbb{R}$, let $v_j = (v, \zeta^j v, \zeta^{2j} v, \dots, \zeta^{(N-1)j} v)^T$ be a vector in $\mathbb{C}$. Suppose $j = 0, \dots, N-1$, then the vectors v_j form a basis for $\mathbb{C}^N$. Observe that the basis decomposes $\mathbb{C}^N$ into $\mathbb{C}^N = V_0 \oplus V_1$, where $V_0 = \{(z_1, \dots, z_N) \in \mathbb{C}^N | z_1 + \cdots + z_N = 0\}$ and $V_1 = \{(z, \dots, z) | z \in \mathbb{C}\}$ are invariant subspaces. Note also that the vectors v_j, with $j = 0$, form a basis for the subspace V_1, while the remaining vectors v_j, $j = 1, \dots, N-1$, form a basis for the subspace V_0.

Since each energy harvester also has an internal phase space of dimension four, we consider again the vectors $v_{ji} = (e_i, \zeta^j e_i, \zeta^{2j} e_i, \dots, \zeta^{(N-1)j} e_i)^T$, which were defined in

§2.4 for the isotypic decomposition of the coupled gyroscope system. We already know that these vectors form a symplectic basis under the symplectic form $\omega(u, v) = u^T J v$, so we leverage the calculations. The corresponding real symplectic transition matrix P is constructed in a similar manner. For complex vector v_{ji}, let $\Re_{ji}$ and $\Im_{ji}$ denote its real and imaginary parts, respectively. Furthermore, we denote a normalized vector by $\tilde{\cdot}$. For N odd, the real symplectic transition matrix is

$$P = \big[\tilde{v}_{01}, \ldots, \tilde{v}_{04}, \widetilde{\Im}_{11}, \widetilde{\Re}_{11}, \ldots, \widetilde{\Im}_{14}, \widetilde{\Re}_{14}, \ldots, \widetilde{\Im}_{\lfloor N/2 \rfloor 1}, \widetilde{\Re}_{\lfloor N/2 \rfloor 1}, \ldots, \widetilde{\Im}_{\lfloor N/2 \rfloor 4}, \widetilde{\Re}_{\lfloor N/2 \rfloor 4}\big].$$

Similarly, the corresponding real symplectic matrix for N even is

$$P = \big[\tilde{v}_{01}, \ldots, \tilde{v}_{04}, \widetilde{\Im}_{11}, \widetilde{\Re}_{11}, \ldots, \widetilde{\Im}_{14}, \widetilde{\Re}_{14}, \ldots, \widetilde{\Im}_{(N/2-1)1}, \widetilde{\Re}_{(N/2-1)1}, \ldots, \widetilde{\Im}_{(N/2-1)4}, \widetilde{\Re}_{(N/2-1)4}, \tilde{v}_{(N/2)1}, \ldots, \tilde{v}_{(N/2)4}\big].$$

From the basis chosen, the complexified phase space can now be written as $\left(\mathbb{C}^N\right)^4 = (V_0)^4 \oplus (V_1)^4$, where $(V_0)^4$ and $(V_1)^4$ are invariant subspaces with respect to ξ.

Applying P to the linear part of (15), we obtain the following diagonalization of the linear part of the coupled energy harvesting array:

$$\mathcal{M} := P^{-1} M P = \operatorname{diag}(\mathcal{M}_0, \mathcal{M}_1, \ldots, \mathcal{M}_1), \tag{16}$$

where $\mathcal{M}_0 = M_1 + (N-1)M_2$ and $\mathcal{M}_1 = M_1 - M_2$.

3.4 *Eigenvalues*

Given the structure of the linear part of the system shown in (16), we only need to study the matrices $\mathcal{M}_0$ and $\mathcal{M}_1$ in order to understand the eigenvalues of the system. The matrix

$$\mathcal{M}_0 = \begin{pmatrix} 0 & -\kappa/2 & 1 & 0 \\ \kappa/2 & 0 & 0 & 1 \\ -1-\kappa^2/4-(n-1)\lambda_r & 0 & 0 & -\kappa/2 \\ 0 & -\beta-\kappa^2/4 & \kappa/2 & 0 \end{pmatrix},$$

has the corresponding characteristic polynomial

$$y^4 + \left(\beta + \kappa^2 + 1 + (N-1)\lambda_r\right) y^2 + \beta + \beta\lambda_r(N-1).$$

Similarly, the matrix

$$\mathcal{M}_1 = \begin{pmatrix} 0 & -\kappa/2 & 1 & 0 \\ \kappa/2 & 0 & 0 & 1 \\ -1-\kappa^2/4+\lambda_r & 0 & 0 & -\kappa/2 \\ 0 & -\beta-\kappa^2/4 & \kappa/2 & 0 \end{pmatrix},$$

has the corresponding characteristic polynomial

$$y^4 + \left(\beta + \kappa^2 + 1 - \lambda_r\right) y^2 + \beta(1-\lambda_r).$$

Observe that the characteristic equations of both matrices, $\mathcal{M}_0$ and $\mathcal{M}_1$, have the same form

$$y^4 + by^2 + c = 0. \tag{17}$$

Thus, we shall first investigate this equation in general and then apply the results to the characteristic equations of the $\mathcal{M}_0$ and $\mathcal{M}_1$ matrices. We start by writing the roots of (17) in the form

$$\pm\sqrt{\frac{-b \pm \sqrt{b^2 - 4c}}{2}}. \tag{18}$$

Since we want the system to be spectrally stable, i.e., all eigenvalues with zero real parts, we need to investigate the following cases separately.

Case 1. $b^2 - 4c > 0$, i.e. $\sqrt{b^2 - 4c} \in \mathbb{R}$

In this case, the roots are purely imaginary if $((-b \pm \sqrt{b^2 - 4c})/2) \leq 0$ or if $c \geq 0$.

For $\mathcal{M}_0$, $c = \beta + \beta\lambda_r(N-1)$. Direct substitution and simplification of the condition $c \geq 0$ leads to the critical value of coupling strength: $\lambda_r \geq -1/(N-1)$. It follows that a bifurcation occurs at the critical value of coupling strength

$$\lambda_c = -\frac{1}{N-1}. \tag{19}$$

For $\mathcal{M}_1$, $c = \beta(1 - \lambda_r)$. Again, substitution into $c \geq 0$ leads to $\lambda_r \leq 1$. It follows that a second bifurcation point occurs at $\lambda_c = 1$. Numerical simulations show that the oscillations that emerge off this point when the forcing term is turned on, have rather small amplitude, i.e., small power output. For this reason, we do not pursue the analysis of this bifurcation any further. For the system with self-coupling, similar calculations show that the bifurcation point with respect to λ_r changes slightly to

$$\lambda_c = -\frac{1}{N}. \tag{20}$$

For the special case of $N = 3$, eq. (20) yields $\lambda_c = -0.333$, which corresponds to the subcritical pitchfork bifurcation identified in figure 5a for a coupled energy harvesting system with zero forcing $F_r = 0$. Observe now in figure 5b that increasing the forcing by a small amount does not lead to a drastic change in the bifurcation point. In fact, numerical simulations show that eq. (19) is a good analytical approximation to the onset of stable synchronized oscillations that emerge through the subcritical pitchfork bifurcation shown in figure 5b.

As λ_r is not part of the characteristic polynomial of $\mathcal{M}_1$, there is no corresponding second bifurcation point in this case.

Case 2. $b^2 - 4c = 0$

In this case, $b \geq 0$ must hold for the eigenvalues to be purely imaginary.

For $\mathcal{M}_0$, $b = \beta + \kappa^2 + 1 + (N-1)\lambda_r$. Direct substitution and simplification of the condition $b \geq 0$ leads to the following critical value of coupling strength:

$$\lambda_r \geq \frac{-\beta - \kappa^2 - 1}{(N-1)}.$$

For $\mathcal{M}_1$, $b = \beta + \kappa^2 + 1 - \lambda_r$. Again, substitution into $b \geq 0$ leads to

$$\lambda_r \leq \beta + \kappa^2 + 1.$$

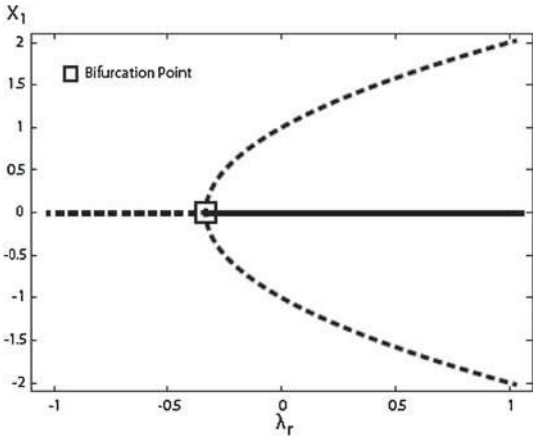

(a) Unforced, $F_r = 0$

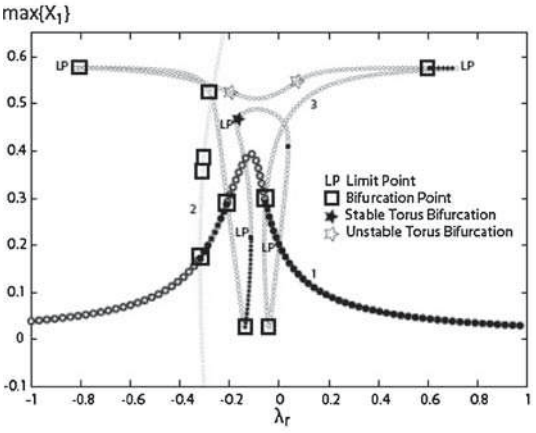

(b) Periodically forced, $F_r = 0.1$

Figure 5. One-parameter bifurcation diagram for a 1D array of $N = 3$ energy harvester beams coupled mechanically and inductively. (**a**) No forcing is applied. (**b**) A sinusoidal forcing term leads to three branches of collective behaviour. Parameters are: $\omega_r = 0.9$, $Q = 100$, $\alpha = 1$, $\kappa^2 = 0.2$, $\gamma = -1$, $\mu = 0.1$. Along Branch 1 complete synchronization, in which all beams oscillate with the same phase and amplitude and same mean values, is obtained. In Branch 2, the beams also oscillate in synchrony but with a non-zero mean. In Branch 3, two of the beams oscillate in phase while the third one oscillates with a different phase.

Case 3. $b^2 - 4c < 0$, i.e., $\sqrt{b^2 - 4c} \in \mathbb{C}$

In this case, the roots can be written as

$$\pm\sqrt{\frac{-b \pm i\sqrt{4c - b^2}}{2}}.$$

In general, the square root of a complex number $v + iw$ can be written as

$$\frac{1}{2}\sqrt{2\sqrt{v^2+w^2}+2v} - \frac{1}{2}icsgn\,(\mp w + iv)\sqrt{2\sqrt{v^2+w^2}-2v}.$$

Thus, in this situation, $v = -(b/2)$ and $w = \sqrt{4c-b^2}/2$. We require that the roots be purely imaginary, yielding

$$\frac{1}{2}\sqrt{2\sqrt{\left(-\frac{b}{2}\right)^2 + \left(\frac{\sqrt{4c-b^2}}{2}\right)^2} + 2\left(-\frac{b}{2}\right)} = 0,$$

which reduces to $4c - b^2 = 0$.

For $\mathcal{M}_0$, $4c - b^2 = 4(\beta + \beta\lambda_r(N-1)) - (\beta + \kappa^2 + 1 + (N-1)\lambda_r)^2 = 0$. Solving for λ_r, we get

$$\lambda_r = \frac{-1 - \kappa^2 + \beta \pm 2\kappa\sqrt{-\beta}}{N-1}.$$

For $\mathcal{M}_1$, $4c - b^2 = 4\beta - 4\beta\lambda - \left(\beta + \kappa^2 + 1 - \lambda\right)^2 = 0$. Again, solving for λ_r, we get

$$\lambda_r = \kappa^2 - \beta + 1 \pm 2\kappa\sqrt{-\beta}.$$

4. Conclusions

Methods from equivariant bifurcation theory were used to study the equations of motion of two network systems: one consisting of vibratory gyroscopes and the other made up of energy harvesters. Under normal conditions of operation, both systems can be treated as Hamiltonian systems with small perturbations. Representation theory allows us to find a suitable basis to study symmetry-breaking bifurcations and stability properties of collective behaviour; in particular, synchronized solution. Furthermore, the analysis yields approximate analytical expressions for the critical coupling strength required to induce synchronization. Future work include experimental realizations of both systems and a comparison of experimental measurements against theory.

Acknowledgements

BC and AP were supported by the Complex Dynamics and Systems Programme of the Army Research Office, supervised by Dr Samuel Stanton, under grant W911NF-07-R-003-4. AP was also supported by the ONR Summer Faculty Research Programme, at SPAWAR Systems Centre, San Diego. VI acknowledges support from the Office of Naval Research, Code 30 under the programme managed by Dr Michael F Shlesinger. P-LB would like to thank Alberto Alinas for checking some early calculations as part of a student project. P-LB acknowledges the funding support from NSERC (Canada) in the form of a Discovery Grant.

References

[1] William Rowan Hamilton, *Philosophical transactions of the Royal Society*, pp 247–308 (1834)
[2] William Rowan Hamilton, *Philosophical Transactions of the Royal Society*, pp 95–144 (1835)
[3] M E Tuckerman, B J Berne and G J Martyna, *J. Chem. Phys.* **94(10)**, 6811 (1991)
[4] N E Leonard and J E Marsden, *Physica D* **105(1–3)**, 130 (1997)
[5] A Bulsara, V In, A Kho, A Palacios, P Longhini, S Baglio and B Ando, *Meas. Sci. Technol.* **19**, 075203 (2008)
[6] V In, A Bulsara, A Palacios, P Longhini, A Kho and J Neff, *Phys. Rev. E* **68**, 045102 (2003)
[7] V In, A Palacios, A Bulsara, P Longhini, A Kho, Joseph Neff, Salvatore Baglio and Bruno Ando, *Phys. Rev. E* **73(6)**, 066121 (2006)
[8] A Palacios, J Aven, P Longhini, V In and A Bulsara, *Phys. Rev. E* **74**, 021122 (2006)
[9] R J McDonald and N Sri Namachchivaya, *Dynam. Stabil. Syst.* **14(4)**, 357 (1999)
[10] R J McDonald and N Sri Namachchivaya, *J. Sound Vib.* **255(4)**, 635 (2002)
[11] R J McDonald, N Sri Namachchivaya and W Nagata, *Fields Institute Commun.* **49**, 79 (2006)
[12] N Sri Namachchivaya and W Nagata, *Proc. R. Soc. London A* **454**, 543 (1998)
[13] L Kocarev and G Vattay, *Complex dynamics in communication networks* (Springer, New York, 2005)
[14] Y Susuki, Y Takatsuji and T Hikihara, *IEICE Trans. Fundamentals* **E92-A(3)**, 871 (2009)
[15] C Acar and A M Shkel, *MEMS Vibratory gyroscopes: Structural approaches to improve robustness* (Springer, 2009)
[16] M S Grewal, L R Weill and A P Andrews, *Global positioning systems, inertial navigation, and integration* (Wiley-Interscience, 2007)
[17] R Rogers, *Applied mathematics in integrated navigation systems* (American Institute of Aeronautics and Astronautics, 2007)
[18] S P Beeby, M J Tudor and N M White, *Meas. Sci. Technol.* **17**, R175 (2006)
[19] F Peano, G Coppa, C Serazio, F Peinetti and A D Angola, *Math. Comput. Model* **43**, 1412 (2006)
[20] V Huy, *Ring of vibratory gyroscopes with coupling along the drive axis*, Ph.D. thesis (San Diego State University, 2011)
[21] Cenk Acar and Andrei Shkel, *MEMS vibratory gyroscopes: Structural approaches to improve robustness* (Springer Verlag, 2009)
[22] Vladislav Apostolyuk, in: *MEMS/NEMS* (Springer, 2006), pp. 173–195
[23] Vladislav Apostolyuk and Francis EH Tay, *Sensor Lett.* **2(3–4)**, 3 (2004)
[24] URL http://en.wikipedia.org/wiki/Coriolis_effect, (2013)
[25] B Dionne, M Golubitsky and I Stewart, *Nonlinearity* **9**, 575 (1996)
[26] Vu Huy, Antonio Palacios, Visarath In, Patrick Longhini and Joseph D Neff, *Chaos* **21(1)**, 013103 (2011)
[27] Vu Huy, Antonio Palacios, Visarath In, Patrick Longhini and Joseph D Neff, *Phys. Rev. E* **81(3)**, 031108 (2010)
[28] P-L Buono, B Chan, A Palacios and V In, *Physica D* (2014) (under review)
[29] S Roundy, P K Wright and J M Rabaey, *Energy scavenging for wireless sensor networks* (Kluwer Academic, Boston, 2004)